

Acta Futura 11 (2018) 37-47

DOI: 10.5281/zenodo.1139226

**Acta
Futura**

GTOC9: Results from the National University of Defense Technology (team NUDT)

YA-ZHONG LUO*, YUE-HE ZHU, HAI ZHU, ZHEN YANG, ZHEN-JIANG SUN, JIN ZHANG

COLLEGE OF AEROSPACE SCIENCE AND ENGINEERING, NATIONAL UNIVERSITY OF DEFENSE TECHNOLOGY
CHANGSHA 410073, CHINA

Abstract. The ninth edition of the Global Trajectory Optimization Competition (GTOC) series was successfully organized in April 2017, wherein the competitors were called to design a series of missions able to remove a set of 123 orbiting debris pieces while minimizing the overall cumulative cost. A three-level optimization framework of the NUDT Team is presented and an improved Ant colony Optimization Algorithm, a hybrid-encoding Genetic Algorithm and an improved Differential Evolution algorithm are applied to solve the complex problem, which combines the dynamic TSP, mixed-integer sequence optimization and perturbed trajectory rendezvous optimization. The result obtained during the competition ranked second in the eventual leaderboard.

1 Introduction

The design of space trajectories can be profitably approached as a global optimization problem. The optimal trajectory, which is significant for practical space mission design, is usually very difficult to be obtained. The Global Trajectory Optimization Competition (GTOC) series [1], was born with the objective of fostering research in this area by letting the

best aerospace engineers and mathematicians worldwide challenge themselves to solve one, difficult, well-defined, problem of spacecraft trajectory design.

Since the launch of the first satellite, Sputnik, in 1957, mankind has placed countless spacecraft in orbit around the Earth. Today, less than 10% of the trackable objects orbiting the Earth are operational satellites. The remainder is simply junk and the space debris is becoming an increasingly serious problem. Following the unprecedented explosion of a Sun-synchronous satellite, the Kessler effect triggered further impacts and the Sun-synchronous orbits environment was severely compromised [2]. Scientists from all main space agencies and private space companies isolated a set of 123 orbiting debris pieces that, if removed, would restore the possibility to operate in that precious orbital environment and prevent the Kessler effect to permanently compromise it.

For calling to protect the environment of earth orbits, the background of GTOC9 is to clean the debris to avoid the Kessler effect. It is the first time that GTOC focuses on the near-earth space problem. The competitors are called to design a series of missions to remove a set of 123 orbiting debris pieces while minimizing the overall cumulative cost.

To find the optimal solution of such a complex problem, three sub-problems need to be extracted and

*Corresponding author. E-mail: luoyz@nudt.edu.cn

solved. First, the set of 123 debris pieces needs to be divided into several groups. Each group of debris is removed by one mission. Optimization is performed to minimize the overall cumulative cost. This can be approached as a dynamic TSP and solved by evolutionary algorithms [3]. Second, given a group of the debris, one mission is designed by mixed-integer optimization to remove them while costing minimal velocity increment [4]. Finally, given the current and next debris as well as the rendezvous duration, the impulsive maneuver strategy is designed to produce the optimal flight trajectory [5].

This paper presents the solving methods and results from the National University of Defense Technology (NUDT) for GTOC9. The remainder of the paper is organized as follows. Section 2 makes a short description of the problem and analyzes the main challenges of this problem. Section 3 gives the optimization framework of the NUDT Team. The detailed solving approach and procedure are presented in Section 4-6. Conclusions are drawn in Section 7.

2 Problem Description and Analysis

2.1 Problem Description

The problem of GTOC9 is to design n missions to cumulatively remove all the 123 orbiting debris while minimizing the overall cumulative cost of such an endeavor. The cost function is expressed as

$$J = \sum_{i=1}^n C_i = \sum_{i=1}^n \left[c_i + \alpha(m_{0i} - m_{dry})^2 \right] \quad (1)$$

$$c_i = c_m + \frac{t_{submission} - t_{start}}{t_{end} - t_{start}} (c_M - c_m)$$

where C_i is the cost charged by the contracted launcher supplier for the i^{th} mission. At the beginning of the i^{th} mission, m_{0i} is the spacecraft mass and m_{dry} its dry mass. Each spacecraft initial mass m_0 is the sum of its dry mass, the weights of the $N \geq 1$ de-orbit packages to be used and the propellant mass: $m_0 = m_{dry} + Nm_{de} + m_p$. α is a parameter set to be $\alpha = 2.0 \times 10^{-6}$ [MEUR/Kg²]. $t_{submission}$ is the epoch at which the i^{th} mission is validated, and t_{end} and t_{start} are the end and the beginning epochs of the GTOC9 competition. The minimal basic cost c_m is 45 MEUR and the maximum cost c_M is 55 MEUR. Other definition and constraints can be found in [2].

During each transfer between two successive debris, the spacecraft dynamics is described by a Keplerian mo-

tion perturbed by main effects of an oblate Earth, i.e. J_2 .

$$\begin{cases} \dot{x} = v_x, & \dot{y} = v_y, & \dot{z} = v_z \\ \dot{v}_x = -\frac{\mu x}{r^3} + \frac{3\mu J_2 R_E^2}{2r^5} \left(\frac{5z^2}{r^2} - 1 \right) x + \Gamma_x \\ \dot{v}_y = -\frac{\mu y}{r^3} + \frac{3\mu J_2 R_E^2}{2r^5} \left(\frac{5z^2}{r^2} - 1 \right) y + \Gamma_y \\ \dot{v}_z = -\frac{\mu z}{r^3} + \frac{3\mu J_2 R_E^2}{2r^5} \left(\frac{5z^2}{r^2} - 3 \right) z + \Gamma_z \end{cases} \quad (2)$$

where $\mathbf{r} = [x, y, z]^T$ and $\mathbf{v} = [v_x, v_y, v_z]^T$ are the spacecraft's position and velocity vector described in the mean equator inertial coordinate system of the center body, $r = \|\mathbf{r}\|$, $\|\cdot\|$ denotes the Euclidean norm of a vector, μ , R_E and J_2 are the gravitational constant, mean equator radius and J_2 -perturbation coefficient of the central body respectively. $\mathbf{\Gamma}$ is the thrust acceleration.

The only maneuvers allowed to control the spacecraft trajectory are instantaneous changes of the spacecraft velocity (its magnitude being denoted by ΔV). After each such maneuver, the spacecraft mass is to be updated using Tsiolkovsky equation:

$$m_f = m_i \exp \left(-\frac{\Delta V}{v_e} \right) \quad (3)$$

where $v_e = I_{sp}g_0$. A maximum of 5 impulsive velocity changes is allowed during each transfer between two successive debris. These do not include the departure and arrival impulse.

2.2 Analysis

The goal of this problem is to design a minimal mass vehicle compliant of a series of successive removal missions. For optimization this problem, three following sub-problems must be addressed:

- 1) How to plan the successive removal missions?
- 2) How to minimize the cost of a single mission?
- 3) How to minimize the trajectory between each two debris?

The first problem is a large-scale multi-sequence combinatorial optimization problem, which is similar to the combination of the classic TSP (Travelling Salesman Problem) and BPP (Bin Packing Problem). The TSP is to find a minimal distance closed path visiting all the nodes once and the BPP is to find a minimal bin-packing scheme placing all the items without omission.

However, compared with TSP and BPP, the following differences make this sub-problems much more difficult to solve.

In the BPP, only the weight constraint need to be satisfied. The placing sequence of each item can be ignore. While in this problem not only the total fuel cost constraint should be satisfied, but also the sequence of the visited debris must be considered. This makes the solution space of this problem much larger than BPP and increase the optimization difficulty.

In the TSP, each node has to be visited once and once only and the path is closed. While removing the debris can be divided into several missions in this problem, where the number of missions are not fixed and the removal paths are opened. This makes the solution space of this problem much larger than TSP and also increase the optimization difficulty.

In the TSP, all the nodes to be visited are fixed in the plane and the cost of going from one node to another can be easily calculated according to the Cartesian distance in the plane. While in this problem the cost of going from a debris to the next one depends on the starting date and arrival date. This makes the problem time-dependent and further increase the optimization difficulty.

The second problem is a mixed-integer nonlinear-programming (MINLP) problem. Not only the sequence of the debris (integer variables) but also the transfer times between each debris (real variables) need to be considered as the Design Variables, which are typically much more difficult to solve than both mixed-integer linear-programming (MILP) and nonlinear-programming (NLP) problems.

The third problem is an orbital transfer problem. It is very difficult to find the optimal solution for the long-duration (t_f is up to 30 days) perturbed rendezvous problem. A fuel-optimal orbital rendezvous problem is to find a maneuvering plan for the spacecraft to minimize the total velocity increment and simultaneously satisfy specific constraints. While the J_2 -perturbation is taken in account, the well-known orbital targeting algorithms such as the Lambert algorithm will be failed in obtaining the feasible solutions, and the constrained optimization methods which can directly corporate final state constraints, such as SQP, will also encounter convergence problems for long-duration rendezvous. From the scope of orbital dynamics, at least two impulses are needed to target the final position and velocity vectors. However, the total velocity increment of the 2-impulse maneuvers will be very large for a rendezvous mission,

especially for the long-duration, large non-coplanar rendezvous. Therefore, a rendezvous mission usually uses more than two impulses. Due to the long-duration, multi-impulse characteristics, the design variables (e.g. the maneuver time) will have large search space, and many sub-optimal solutions may exist, thus it is difficult to find the global optimal solution for this problem even though the state-of-art optimization algorithm is used. In addition, numerical integration of the J_2 -perturbed trajectory is required in the optimization process, which makes the optimization time-consuming.

3 Optimization framework

Based on the analysis of the problem and the optimization tools we have accumulated, our optimization framework is divided into three levels, which are illustrated in Fig. 1.

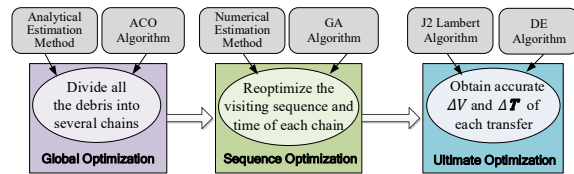


FIGURE 1. Optimization framework

The task of the global optimization is to appropriately divide the debris into several chains. It is a combinatorial optimization problem with huge search space that is similar to the TSP. For such NP-hard problem, no algorithm can guarantee to the global optimum. As an efficient optimization tool, ACO performs well on the classic TSP and many other TSP variants. Following the characteristic of this problem, we improve an ACO based on the one for the extravehicular missions packing programming (EMPP) [6] and apply it to solve the first-level problem. In addition, compared with the calculating of the distance between any two cities in the TSP, the calculating of the ΔV from a debris to the next one is much more time-consuming. Thus, an analytical estimation method of the transfer ΔV and ΔT between any two debris is employed in the global optimization.

With the completion of the global optimization for the whole mission, the number of the chains and the debris in each chain are determined and will not be changed. However, since the optimal transfer ΔV and ΔT between each debris are estimated by an analytical model with high error (up to 30% in some conditions),

a numerical estimation method of the transfer ΔV and ΔT between any two debris is developed and the mixed integer reoptimization for both the visiting sequence of the chain and the transfer time between each debris is necessary. An improved hybrid-encoding Genetic Algorithm (HEGA) [7, 8] is applied to solve the second-level problem.

Once the visiting sequence of each chain is determined, the optimization of the accurate transfer ΔV and ΔT between each two debris is required. The orbital transfer from a debris to another is a multi-impulse, perturbed rendezvous problem. A feasible solution cannot be directly obtained by the orbital targeting algorithms based on two-body dynamics unless some differential corrections or simple iterations are used. In order to efficiently obtain a near-optimal solution for the given long-duration (up to 30 days) rendezvous

problem, a feasible iteration optimization model is employed, in which the homotopic perturbed Lambert algorithm [9, 10] is used as the orbital targeting algorithm. An improved differential evolution (DE) algorithm [11] is applied to solve the third-level problem.

4 Global Optimization for the Whole Mission

4.1 Analytical estimation method of the transfer ΔV and ΔT

The analytical estimation method for evaluating the objective function of each transfer and the overall cumulative cost are based on the Gauss form of variational equations [12],

$$\begin{cases} \Delta a = \frac{2}{n\sqrt{1-e^2}} [e \sin f \cdot \Delta v_r + (1 + e \cos f) \Delta v_t] \\ \Delta e = \frac{\sqrt{1-e^2}}{na} [\sin f \cdot \Delta v_r + (\cos f + \cos E) \Delta v_t] \\ \Delta i = \frac{na}{r \cos u} \Delta v_h \\ \Delta \Omega = \frac{r \sin u}{na^2 \sqrt{1-e^2} \sin i} \Delta v_h \\ \Delta \omega = \frac{\sqrt{1-e^2}}{nae} \left[-\cos f \cdot \Delta v_r + \left(1 + \frac{r}{p}\right) \sin f \cdot \Delta v_t \right] - \cos i \cdot \Delta \Omega \\ \Delta M = n - \frac{1-e^2}{nae} \left[\left(2e \frac{r}{p} - \cos f\right) \Delta v_r + \left(1 + \frac{r}{p}\right) \sin f \cdot \Delta v_t \right] \end{cases} \quad (4)$$

where the mean motion $n = \sqrt{\frac{\mu}{a^3}}$ and the semilatus rectum $p = a(1 - e^2)$. Detailed procedure is described as follows.

1) Adjustment of the RAAN difference

The RAAN of an orbital object drifts due to the J_2 perturbation. The drift velocity is formulated as follow,

$$\dot{\Omega} = -\frac{3}{2} J_2 \left(\frac{r_{eq}}{p} \right)^2 n \cos i \quad (5)$$

where r_{eq} is the mean radius of the earth.

As the adjustment of orbital plane costs a large velocity increment, the difference of the RAAN drift velocity between the spacecraft and the debris should be fully used. If the RAAN difference cannot be remedied naturally during the maximum rendezvous duration, an impulse perpendicular to the orbital plane can be implemented at the north or south vertex of the orbit.

$$\Delta v_h = \frac{na^2 \sqrt{1-e^2} \sin i}{r} |\Delta \Omega| \quad (6)$$

2) Adjustment of the inclination difference

As the J_2 perturbation does not change the orbital inclination, the inclination difference must be remedied by maneuvers. An impulse perpendicular to the orbital plane can be implemented at the ascending node or descending node.

$$\Delta v = 2 \frac{h}{r} \sin \frac{|\Delta i|}{2} \quad (7)$$

where $h = r^2 \dot{\theta}$, θ is the argument of latitude.

3) Adjustment of the semimajor axis and eccentricity

After the spacecraft transfers to the same orbital plane with the debris, the semimajor axis and eccentricity are adjusted by two tangential impulses. For a near circular orbit, omitting the high order terms of e^2 , the impulses are formulated as follows.

If $\Delta a \Delta e \geq 0$, the first tangential impulse Δv_{t1} is implemented at the perigee, where the true anomaly $f = 0$, and the second tangential impulse Δv_{t2} is implemented at the apogee of $f = \pi$.

$$\begin{cases} \Delta v_{t1} = n \frac{\Delta a + a(1-e)\Delta e}{4} \\ \Delta v_{t2} = n \frac{\Delta a - a(1+e)\Delta e}{4} \end{cases} \quad (8)$$

If $\Delta a \Delta e < 0$, the first tangential impulse Δv_{t1} is implemented at the apogee, where the true anomaly $f = \pi$, and the second tangential impulse Δv_{t2} is implemented at the perigee of $f = 0$.

$$\begin{cases} \Delta v_{t1} = n \frac{\Delta a - a(1+e)\Delta e}{4} \\ \Delta v_{t2} = n \frac{\Delta a + a(1-e)\Delta e}{4} \end{cases} \quad (9)$$

4) Estimation of rendezvous duration

The rendezvous duration should mainly come from the adjustment of the RAAN difference so as to make full use of the natural RAAN drift due to J_2 perturbation. The other adjustments do not need too much time. To be conservative, the rendezvous duration is roughly estimated as the duration for RAAN adjustment plus one day.

4.2 ACO for Debris Grouping and Bunching

ACO algorithm was originally inspired by the ability of biological ants to find the shortest path between their nest and a food source [13]. The fundamental working procedure of the ACO for debris Grouping and bunching (ACO_DGB) is similar to the classic ACO, which is shown in Algorithm 1. The most important feature of an ACO is the design of the heuristic, which is eventually combined with the pheromone information to build solutions. In this part, we mainly present the heuristic and solution construction method of the DCB_ACO.

Algorithm 1 Ant System

step 1: Pheromone trail initialization;
while termination criteria not met
do
 step 2: Solution construction;
 step 3: Pheromone update;
end while

The procedure of bunching a debris chain is illustrated in Fig. 2. After setting the start time and select a debris as the head of the chain, the estimation of the optimal transfer ΔV and ΔT between the last debris of the current chain and all remaining ones and the selection from the candidate pool are followed and cycled to bunch the chain one by one. When the candidate pool

becomes empty, which means none of the remaining debris can be added to the tail of the chain, the procedure will be stopped and a chain will be obtained.

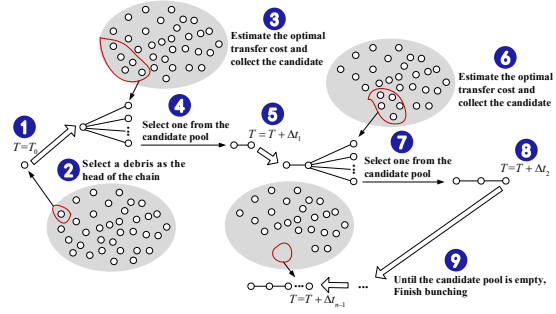


FIGURE 2. Bunching procedure of the debris chain

Three remarks should be noted for this procedure:

- 1) In steps 3 and 6, the candidate refers to all of the debris that satisfy the total fuel constraints for one mission after being added to the tail of the chain.
- 2) In steps 4 and 7, the probability that an ant k will choose a debris j as the next debris for the current chain b in the partial solution s is given by

$$p_{bj}^k(s) = \begin{cases} \frac{\tau_{bj} \cdot \eta_j^\beta}{\sum_{g \in U^k(s,b)} \tau_{bg} \cdot \eta_g^\beta}, & j \in U^k(s,b) \\ 0 & otherwise \end{cases} \quad (10)$$

where $U^k(s, b)$ is the candidate pool and $\eta_j = \Delta V_{lj}$ is the heuristic value. The parameter α in the classic ACO is fixed to 1 here because using the parameter β is sufficient to reflect the weight between the pheromone information and heuristic information. τ_{bj} is the pheromone from debris l to debris j , where debris l is the last debris in the current chain b .

- 3) In step 5 and 8, δt is the estimated optimal transfer time between the last debris in the current chain and the selected debris.

Based on the chain bunching method, building a solution for each ant should take the following procedure, which is presented as Algorithm 2.

Algorithm 2 Solution Construction Procedure of the ACO_DGB

step 1: Determine the start time T_0 (MJD)

- step 2: Produce a debris chain based on the chain bunching method in Fig. 2
- step 3: **if** None debris remains
Go to step 4
else
Set the current time $T = T + \Delta T_M$ ($\Delta T_M \in \text{rand}[30\text{day}, 60\text{day}]$)
Return to step 2
end if
- step 4: Collect all of the debris chains and obtain a solution

The evaporation parameter ρ is set as 0.05 and the increase of the pheromone $\Delta\tau_{ij}^k$ is limited to the maximum value of $0.1\tau_{ij}^k$ to avoid premature convergence. The pheromone update rule used in the ACO_DGB is the same as the one in the ACO for the EMPP [6].

4.3 Solving Strategy

To minimize the cost function that is expressed in Eq. (1), not only the launch times but also the total propellant cost in each launch should be reduced. The time-related part c_i is set as the maximum cost (55 MEUR) in the optimization for the whole mission.

Due to the insufficient optimization performance of the ACO_DGB, we can hardly obtain the optimal solution or even a good solution if using the algorithm to optimize 123 debris all at once and taking the solution from the result directly. In order to make the original problem easier to be optimized and obtain better solutions, a chain-by-chain solving strategy is applied, which is illustrated in Fig. 3.

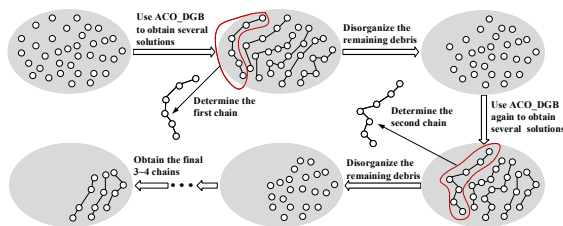


FIGURE 3. Procedure of the chain-by-chain solving strategy

The main idea of this solving strategy is to determine the debris chains of the final solution step by step. 2000 runs will be implemented for the ACO_DGB to optimize the remaining debris each time and the first chain of the best partial solution will be selected and

determined as the next chain of the final solution. Here the best partial solution refers to the one that owns the smallest objective function value excluding the determined chains. The final 3-4 chains are determined all at once because the search space is small enough and further disorganization and reoptimization for the remaining debris will not make the final solution better.

5 Sequence Optimization for the Debris Chain

5.1 Optimization Model

1) Design variables

The solution of a debris chain \mathbf{Y} is made up of a group of serial integers \mathbf{Y}_1 and a set of real numbers \mathbf{Y}_2 .

$$\mathbf{Y} = (\mathbf{Y}_1, \mathbf{Y}_2) \quad (11)$$

where \mathbf{Y}_1 refers to the rendezvous sequence (p_1, p_2, \dots, p_Q) , and \mathbf{Y}_2 refers to the orbital transfer time $(dur_1, dur_2, \dots, dur_Q)$.

Through the sequence of its elements the serial integer vector \mathbf{Y}_1 represents a rendezvous order. The search space of \mathbf{Y}_1 is therefore discrete and its elements must be manipulated in combination.

2) Objective function

The objective is to minimize the propellant consumed by orbital maneuvers:

$$\min f_2 = (m_0 - m_{dry} - Qm_{de}) \quad (12)$$

where m_{dry} is the spacecraft's mass after the last removing mission and also denotes the spacecraft's dry mass (Generally, m_{dry} should include the propellant used by spacecraft to deorbit, otherwise, the spacecraft itself would be a debris now).

5.2 Numerical estimation method of the transfer ΔV and ΔT

The state of a spacecraft can be expressed as

$$\mathbf{E} = (a, u, \xi, \eta, i, \Omega)^T \quad (13)$$

where a is the semi-major axis, i is the orbital inclination, Ω is the right ascension of ascending node (RAAN), u is the argument of latitude, e is the eccentricity, ω is the argument of perigee, and $\xi = e \cos \omega$ and $\eta = e \sin \omega$ are the modified orbital elements suitable for de-scribing near-circular orbits.

The state variable used to express orbital differences between the spacecraft and a debris is

$$\mathbf{X} = (\Delta a/a_r, \Delta\theta, \Delta\xi, \Delta\eta, \Delta i, \Delta\Omega)^T \quad (14)$$

where the subscript r denotes the reference orbit, Δa is the difference in semi-major axis, $\Delta\theta$ is the difference

in argument of latitude, Δi is the difference in orbital inclination, $\Delta\Omega$ is the difference in RAAN, and $\Delta\xi$ and $\Delta\eta$ give the differences in eccentricity vector.

Using the first order approximations, the state transitions of the orbital element differences under the J_2 perturbation are given by [10]

$$\begin{cases} \Delta a = \Delta a_0 \\ \Delta\theta = \Delta\theta_0 - \left[\frac{3}{2}n_r \frac{\Delta a_0}{a_r} + \frac{7}{2} \frac{\Delta a_0}{a_r} C(3 - 4\sin^2 i_r) \right] \Delta t - 4C \sin(2i_r) \Delta i_0 \Delta t \\ \Delta\xi = \Delta\xi_0 \cos(\dot{\omega}_{J_2} \Delta t) - \Delta\eta_0 \sin(\dot{\omega}_{J_2} \Delta t) \\ \Delta\eta = \Delta\xi_0 \sin(\dot{\omega}_{J_2} \Delta t) + \Delta\eta_0 \cos(\dot{\omega}_{J_2} \Delta t) \\ \Delta i = \Delta i_0 \\ \Delta\Omega = \Delta\Omega_0 + \left(\frac{7}{2} \frac{\Delta a_0}{a_r} \cos i_r + \sin i_r \Delta i_0 \right) C \Delta t \end{cases} \quad (15)$$

where the subscript 0 denotes the initial state, Δt is the orbital transfer time, μ is the geocentric gravitation constant, a_e is the mean equatorial radius of the Earth, $n_r = \sqrt{\frac{\mu}{a_r^3}}$ is the mean angular motion rate,

$C = \frac{3J_2 a_e^2}{2} \sqrt{\mu} a_r^{-\frac{7}{2}}$, and $\dot{\omega}_{J_2} = C(2 - \frac{5}{2}\sin^2 i_r)$ is the drift rate of perigee.

Thus, the orbital transfer of the q^{th} rendezvous operation can be expressed as

$$\mathbf{X}(t_{qf}) = \Phi(\Delta t_{q0}) \mathbf{X}_0 + \sum_{j=1}^2 \Phi_v(\Delta t_{qj}, u_{qj}) \Delta \mathbf{v}_{qj} \quad (16a)$$

$$\Phi(\Delta t_{q0}) = \begin{bmatrix} 1 & 0 & 0 & 0 & 0 & 0 \\ \left(-\frac{3}{2}n_r \Delta t_{q0} - \frac{7}{2}C \left(\frac{3-4\sin^2 i_r}{4\sin^2 i_r} \right) \Delta t_{q0} \right) & 1 & 0 & 0 & -4C \sin(2i_r) \Delta t_{q0} & 0 \\ 0 & 0 & \cos \tau_{q0} & -\sin \tau_{q0} & 0 & 0 \\ 0 & 0 & \sin \tau_{q0} & \cos \tau_{q0} & 0 & 0 \\ 0 & 0 & 0 & 0 & 1 & 0 \\ \frac{7}{2}C \cos i_r \Delta t_{q0} & 0 & 0 & 0 & C \sin i_r \Delta t_{q0} & 1 \end{bmatrix} \quad (16b)$$

$$\Phi_v(\Delta t_{qj}, u_{qj}) = \begin{bmatrix} 0 & 2 & 0 \\ 0 & \begin{bmatrix} -3n_r - \frac{7}{2}C \left(\frac{3-4\sin^2 i_r}{4\sin^2 i_r} \right) \end{bmatrix} \Delta t_{qj} & -4C \sin(2i_r) \cos u_{qj} \Delta t_{qj} \\ \sin(u_{qj} + \tau_{qj}) & 2 \cos(u_{qj} + \tau_{qj}) & 0 \\ -\cos(u_{qj} + \tau_{qj}) & 2 \sin(u_{qj} + \tau_{qj}) & 0 \\ 0 & 0 & \cos u_{qj} \\ 0 & 7C \cos i_r \Delta t_{qj} & \left(\frac{\sin u_{qj}}{C \sin i_r} + \cos u_{qj} \Delta t_{qj} \right) \end{bmatrix} \quad (16c)$$

where $\tau_{qj} = \dot{\omega}_{J_2} \Delta t_{qj}$, $\Delta t_{q0} = t_{qf} - t_{q0} = dur_q$ is orbital transfer time, $\Delta t_{qj} = t_{qf} - t_{qj}$, u_{qj} is the argument of latitude of the j^{th} maneuver, and $\Delta \mathbf{v}_{qj} = (\Delta v_{qjx}, \Delta v_{qjy}, \Delta v_{qjz})^T$ is the impulse vector. The orbital coordinate system used to describe the impulse is given as follows: x is along the orbital radial direction, y is along the in-track direction and z is along the orbital normal direction and completes the right-handed system. The last maneuver is executed at t_{qf} , i.e. $t_{qf} = t_{q2}$.

Eq. (16) is a linear relative dynamic equation under the J_2 perturbation. Only two maneuvers are considered for each orbital transfer that six unknown impulse components correspond to six equations, and then the solution to Eq. (16) can be easily obtained using Gaussian elimination. The details of this linear dynamics model can be found in the references [14, 15].

Long-duration rendezvous problems under the J_2 perturbation have multiple local minima both in the duration of one orbital period and in the duration of multiple orbital period [15]. In order to overcome the property of multiple local minima in one orbital period, the burn time of the first maneuver t_{q1} is enumerated from t_{q0} to $t_{q0} + T_r$ with a step of T_r/N_{enum} , where T_r is the reference orbital period and N_{enum} is the number of enumerations. For each value of t_{q1} , a group of values for $\Delta \mathbf{v}_{q1}$ and $\Delta \mathbf{v}_{q2}$ can be obtained, and is referred to as $\Delta \mathbf{v}_{q1}(t_{q1})$ and $\Delta \mathbf{v}_{q2}(t_{q1})$. The $N_{enum} + 1$ groups of $\Delta \mathbf{v}_{q1}(t_{q1})$ and $\Delta \mathbf{v}_{q2}(t_{q1})$ in total are calculated and then are compared with each other to find the group with the local minimum value of $\|\Delta \mathbf{v}_{q1}(t_{q1})\| + \|\Delta \mathbf{v}_{q2}(t_{q1})\|$, and the values of the $\Delta \mathbf{v}_{q1}$ and $\Delta \mathbf{v}_{q2}$ in this group are used as the impulses for the orbital transfer of the q^{th} rendezvous.

Based on the method provided above, the maneuver impulses of each rendezvous orbital transfer are only functions of the initial state, the required ending state and the orbital transfer time, and then the propellant cost can be evaluated with small computation cost.

6 Optimization for the Debris-to-debris Transfer

6.1 Optimization Model

1) Design variables

$4n$ design variables are contained in an n -impulse maneuver plan:

$$\mathbf{D} = [t_i, \Delta v_{ix}, \Delta v_{iy}, \Delta v_{iz}], \quad i = 1, 2, \dots, K \quad (17)$$

where K is the total number of the maneuvers, t_i is the i^{th} maneuver time and $\Delta \mathbf{v}_i = [\Delta v_{ix}, \Delta v_{iy}, \Delta v_{iz}]^T$ is the i^{th} maneuver impulse vector. Herein, 4-impulse maneuver plan is adopted.

2) Objective function

The objective is to minimize the total velocity increment:

$$\min J = \Delta v = \sum_{i=1}^K \|\Delta \mathbf{v}_i\| \quad (18)$$

3) Constraints

The duration between two adjacent maneuvers should be larger than a given value, i.e.,

$$\begin{cases} t_i - t_{i-1} \geq \Delta T_i, \\ t_i \in [t_0, t_f], \quad i = 1, 2, \dots, K \end{cases} \quad (19)$$

where $t_0 = 0$, $t_f = 30$ days, $\Delta T_1 = 5$ days, ΔT_i can be set as zeros for $i = 2, \dots, K$. In addition, at the final time, the deviation between the spacecraft's state vector $\mathbf{x}_f = [r_f, v_f]^T$ and the state vector \mathbf{x}_{next} of the next debris should be smaller than the given tolerant error, i.e.,

$$\begin{cases} \|\mathbf{r}_f - \mathbf{r}_{next}\| \leq 100 \text{ m}, \\ \|\mathbf{v}_f - \mathbf{v}_{next}\| \leq 1 \text{ m/s} \end{cases} \quad (20)$$

6.2 Feasible Solution Iteration Optimization Approach

Based on the impulsive maneuver assumption, a feasible solution iteration approach is used to solve this optimization problem, which can be divided into the following two parts.

1) Dealing with the Linear Constraints

A group of proportionality coefficients $\eta_1, \dots, \eta_K \in [0, 1]$ is used to substitute the maneuver times t_1, \dots, t_K as optimization variables. Then, the maneuver times can be calculated as

$$\begin{cases} t_i = t_{i-1} + \eta_i(t_f - t_{i-1}) + \Delta T_i \\ \Delta T_1 = 5 \text{ days}, \\ \Delta T_i = 0, \quad i = 2, \dots, K \end{cases} \quad (21)$$

2) Dealing with the Nonlinear Constraints

The last two impulses $\Delta \mathbf{v}_{K-1}$ and $\Delta \mathbf{v}_K$ are chosen to satisfy the nonlinear equality constraints, and that they are obtained by solving a perturbed two-point

boundary value problem. Otherwise, the number of design variables in Eq. (17) is reduced to $4K - 6$, and the equation can be expressed as

$$\mathbf{X} = [\eta_1, \dots, \eta_K, \Delta \mathbf{v}_1, \dots, \Delta \mathbf{v}_{K-2}] \quad (22)$$

After the proportionality coefficients and the first $K - 2$ nominal impulses $\Delta \mathbf{v}_i$ ($i = 1, 2, \dots, K - 2$) are provided by the optimization algorithm, the maneuver time can be computed using Eq. (21).

Then the spacecraft's trajectory is propagated to t_{K-1} by substituting $\Delta \mathbf{v}_i$ ($i = 1, 2, \dots, K - 2$) into the dynamics of Eq. (2), and the spacecraft's state $\mathbf{x}(t_{K-1})$ can be obtained. Following this, the last two nominal impulses are computed by solving a two-point boundary value problem so that the final rendezvous conditions of Eq. (20) can be automatically satisfied. Here the homotopic perturbed Lambert algorithm proposed by Yang et al. [10] is used to calculate these two impulses as described by:

$$(\Delta v_{K-1}, \Delta v_K) = \text{Lambert}_p((t_{K-1}), \mathbf{x}(t_K), t_K - t_{K-1}) \quad (23)$$

where $\mathbf{x}(t_K) = \mathbf{x}_{\text{next}}$, and the position and velocity error tolerances for the perturbed Lambert algorithm are respectively set as 100 m and 1 m/s. This perturbed Lambert algorithm allowed the perturbed solutions that included the successful computation of the gravitational potential terms J_2 through a homotopic targeting technique in which the two-body Lambert solution is used as an initial value and the Runge-Kutta integration is used as a perturbed trajectory propagator. A set of middle target points along the position offset vector (i.e., the offset between the initial and the final perturbed trajectories) is chosen to approach the final target point iteratively so that the iteration from two-body Lambert solution can converge for this long-duration, multi-revolution Lambert problem.

7 Results

Table 1 presents the best solution we obtained during the competition, in which the start and end epoch as well as the sequence and the start mass of each mission are listed. It can be found that the number of the removal debris in each mission are mainly distributed from seven to twelve except for the first mission.

The total velocity increments for rendezvous of each mission are presented in Fig. 4. It can be seen that the total velocity increments of most missions are between 1500 m/s and 2500 m/s while only that of the fifth mission is beyond 3000 m/s. However, it should be noticed that the first mission has also removed the most debris. Consequently, the average velocity increments of each mission are better indexes to evaluate the perfor-

mance of each mission, which are shown in Fig. 5. We find that the average velocity increments of the first four missions are below 250 m/s while for most of other missions the average velocity increments are near 300 m/s. It indicated that the performances of the first four missions are better than others. It is clear that the average velocity increment of the eighth mission is the largest with a number of near 400 m/s, which indicates that the mission is not optimal. The minimum and maximum velocity increments of each mission are illustrated in Fig. 6. The smallest velocity increment of all 12 missions is 38.6 m/s while the largest one is 798.3 m/s. It can be seen that the range of velocity increments for a single rendezvous process of each mission is very wide.

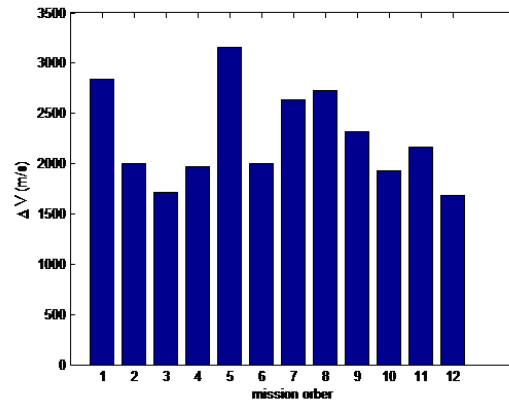
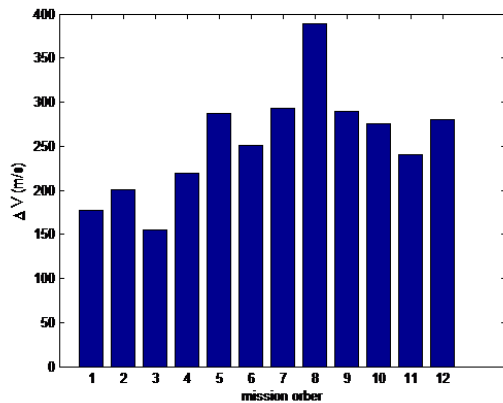
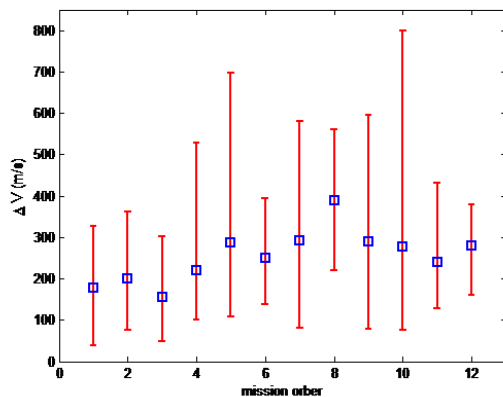


FIGURE 4. Total ΔV of each mission

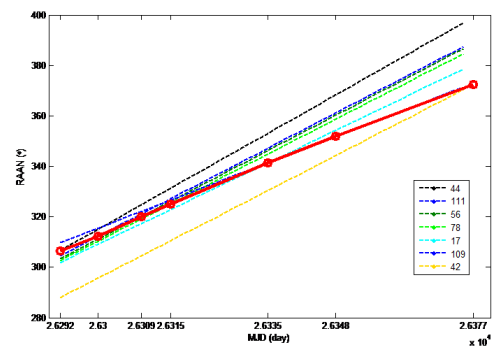
The histories of the RAAN of the active spacecraft

TABLE 1. Details of the best solution from NUDT

Mission Order	Start Epoch (MJD)	End Epoch (MJD)	Debris Number	Debris Removal Sequence	Start Mass (kg)
1	23517.00	23811.52	17	0, 115, 12, 67, 19, 48, 122, 7, 63, 61, 82, 107, 41, 11, 45, 85, 47	5478.12
2	23893.80	24092.29	11	58, 28, 90, 51, 72, 69, 10, 66, 73, 64, 52	4106.88
3	24122.30	24427.74	12	84, 86, 103, 16, 121, 92, 49, 23, 20, 54, 27, 36	3809.97
4	24461.50	24660.15	10	8, 43, 9, 55, 95, 14, 102, 39, 113, 110	4081.09
5	24785.00	24975.41	12	83, 75, 22, 35, 119, 24, 108, 37, 112, 104, 32, 114	5782.68
6	25006.00	25198.32	9	118, 65, 74, 50, 94, 21, 97, 79, 120	4024.43
7	25281.60	25454.87	10	62, 1, 40, 76, 89, 99, 15, 59, 98, 116	4877.61
8	25555.40	25669.64	8	117, 91, 93, 70, 18, 105, 88, 46	4909.98
9	25702.40	25860.22	9	5, 53, 33, 68, 71, 80, 57, 60, 106	4419.99
10	25912.74	26055.85	8	2, 81, 96, 6, 100, 30, 34, 26	3902.24
11	26087.53	26262.18	10	87, 29, 101, 31, 38, 25, 4, 77, 13, 3	4267.35
12	26292.26	26381.58	7	44, 111, 56, 78, 17, 109, 42	3584.37

**FIGURE 5.** Average ΔV of each mission**FIGURE 6.** Minimum and maximum ΔV of each mission

and corresponding debris removed in the last mission are shown in Fig. 7, where the red line with circles indicated the history of RAAN of the spacecraft. We can find that the RAAN of the spacecraft increases gradually as it rendezvouses the debris one by one. The RAAN of debris #42, as shown in the figure, is not close to others in this sequence. However, there is an intersection of the RAAN between debris #42 and debris #109 around 26377 MJD. Thus, the spacecraft can wait to transfer from debris #42 to debris #109 until to that epoch so as to reduce the velocity increments for maneuvers caused by a large initial RAAN error.

**FIGURE 7.** History of the RAAN of the active spacecraft and corresponding debris for mission #12

8 Conclusions

A three-level optimization framework is presented to solve the problem of GTOC9, wherein the competitors

are called to design a series of missions able to remove a set of 123 orbiting debris pieces while minimizing the overall cumulative cost. The top level is similar to a dynamic TSP, wherein the debris pieces are divided into several groups and each group of debris is removed by one mission. The middle level is a mixed-integer optimization problem, wherein the impulses and durations of each rendezvous in one mission are designed. And the bottom level is the precise and detailed optimization of the flight trajectory in one rendezvous. The result of GTOC9 obtained by this framework is then illustrated. The result indicates that the three-level optimization framework is efficient and can obtain good solutions in considerable time.

Acknowledgement

The NUDT team thanks the Advanced Concepts Team of the European Space Agency for organizing such a wonderful GTOC. The innovation of the real-time leaderboard makes GTOC9 more exciting than the past edition and the interesting problem brings us many ideas for further research.

References

- [1] GTOC Portal. https://sophia.estec.esa.int/gtoc_portal/.
- [2] D. Izzo and M. Märten. The Kessler Run: On the Design of the GTOC9 Challenge. *Acta Futura*, pages 11–24, 2018.
- [3] D. Izzo, I. Getzner, D. Hennes, and L. F. Simes. Evolving solutions to TSP variants for active space debris removal. In *Proceedings of the 2015 Annual Conference on Genetic and Evolutionary Computation, GECCO*, pages 1207–1214. ACM Press, 2015.
- [4] J. Zhang, G. T. Parks, Y. Z. Luo, and G. J. Tang. Multispacecraft refueling optimization considering the J2 perturbation and Window Constraints. *Journal of Guidance, Control, and Dynamics*, 37(1):111–122, 2014.
- [5] Y. Z. Luo, G. J. Tang, Y. J. Lei, and H. Y. Li. Optimization of Multiple-Impulse, Multiple-Revolution, Rendezvous-Phasing Maneuvers. *Journal of Guidance, Control, and Dynamics*, 30(4):946–952, 2007.
- [6] Y. H. Zhu, Y. Z. Luo, K. C. Tan, and X. Qiu. An Intelligent Packing Programming for Space Station Extravehicular Missions. *IEEE Computational Intelligence Magazine*, 12(4):38–47, 2017.
- [7] S. Chatterjee, C. Carrera, and L. A. Lynch. Genetic algorithms and traveling salesman problems. *European Journal of Operational Research*, 93(3):490 – 510, 1996.
- [8] K. Deb and A. Pratap and S. Agarwal and T. Meyarivan. A fast and elitist multiobjective genetic algorithm: NSGA-II. *IEEE Transactions on Evolutionary Computation*, 6(2):182–197, 2002.
- [9] Z. Yang, Y. Z. Luo, and J. Zhang. Robust Planning of Nonlinear Rendezvous with Uncertainty. *Journal of Guidance, Control, and Dynamics*, 40(8):1954–1967, 2017.
- [10] Z. Yang, Y. Z. Luo, J. Zhang, and G. J. Tang. Homotopic Perturbed Lambert Algorithm for Long-Duration Rendezvous Optimization. *Journal of Guidance, Control, and Dynamics*, 38(11):2215–2223, 2015.
- [11] Y. H. Zhu, H. Wang, and J. Zhang. Spacecraft Multiple-Impulse Trajectory Optimization Using Differential Evolution Algorithm with Combined Mutation Strategies and Boundary-Handling Schemes. *Mathematical Problems in Engineering*, 2015:1–13, 2015.
- [12] Y. Z. Luo, H. Y. Li, and G. J. Tang. Hybrid Approach to Optimize a Rendezvous Phasing Strategy. *Journal of Guidance, Control, and Dynamics*, 30(1):185–191, 2007.
- [13] M. Dorigo and L. M. Gambardella. Ant colony system: a cooperative learning approach to the traveling salesman problem. *IEEE Transactions on Evolutionary Computation*, 1(1):53–66, 1997.
- [14] P. Labourdette and A. A. Baranov. Strategies for on-orbit rendezvous circling Mars. *Advances in the Astronautical Sciences*, 109:1351–1368, 2002.
- [15] J. Zhang, Y. Z. Luo, and G. J. Tang. Hybrid planning for LEO long-duration multi-spacecraft rendezvous mission. *Science China Technological Sciences*, 55(1):233–243, 2012.
